Vacancy and Cation Distribution in Yttria-Doped Ceria: An ^{89}Y and ^{17}O MAS NMR Study

Namjun Kim* and Jonathan F. Stebbins

Department of Geological and Environmental Sciences, Stanford University, Stanford, California 94305-2115

Received June 8, 2007. Revised Manuscript Received August 27, 2007

The local structure and dynamics of oxide ions in yttria-doped ceria (YDC, 5 to 30% Y_2O_3) were studied using high-resolution ^{89}Y and ^{17}O MAS NMR spectroscopy at ambient temperature and high temperatures to 500 °C. Eight-, seven-, and six-coordinated yttrium cations are clearly resolved in ^{89}Y MAS NMR spectra, and their relative populations were measured. The derived average coordination number of yttrium is smaller than that for a random distribution of oxygen vacancies, suggesting that there is strong association between yttrium cations and vacancies and there is the possibility of pairing of two yttrium cations with one vacancy. In the ^{17}O MAS NMR spectra, resonances for oxygens with different coordination environments are resolved and are assigned to oxygens with different numbers of yttrium cations in the first coordination sphere. The relative intensities of the ^{17}O resonances also deviate from those expected from a random distribution, again indicating possible pairing of yttrium cations. High-temperature ^{17}O MAS NMR shows coalescence among various peaks. The exchange between oxygen sites with yttrium neighbors appears to occur at a lower temperature (about 100 °C) than the exchange that involves the sites without yttrium neighbors; rapid exchange of all oxide anions throughout the structure occurs above 400 °C.

Introduction

Among various types of fuel cells, those with solid oxide electrolytes (SOFCs) have some advantages such as high efficiency and materials compatibility. Although yttria-stabilized zirconia (YSZ) is widely used as an electrolyte due to its outstanding chemical and mechanical stabilities, it requires temperatures up to 1000 °C to achieve sufficiently high conductivity. High operating temperature has limited the application of YSZ-based SOFCs in areas such as transportation and portable electronic devices; high costs of other components and maintenance due to aging and degradation have also been significant to more widespread applications such as medium-sized power generation units. Therefore, development of solid electrolytes that can be used in intermediate temperature ranges (e.g., 600−800 °C) is important for the future growth of SOFC technology.

Doped ceria is one of the most promising electrolyte materials for solid oxide ionic devices operating at intermediate temperatures, because it can have conductivity 1 or 2 orders of magnitude higher than most widely used stabilized zirconias.[1−3] Both types of materials have the same fluorite cubic structure. Although ceria is also commonly doped with aliovalent cations to generate oxygen vacancies and thus improve the ionic conductivity, unlike zirconia it does not require a dopant to be stabilized in the cubic structure. Therefore, cubic fluorite phase doped ceria is stable over a wide range of temperature and dopant concentrations. There may thus be fewer problems in long term applications from the growth of minor ordered phases, which appear to be one of the causes of degradation of zirconia. In spite of the higher conductivity, doped cerias can have different problems such as instabilities caused by changes of unit cell size resulting from formation of Ce^{3+} in high-temperature reducing environments, and associated electronic conduction.[3−5]

Ceria is commonly doped with Ln^{3+} ($Y^{3+}$and other lanthanides); Sm- and Gd-doped (SDC, GDC) ceria are known to have the highest conductivities. Among these materials, the conductivity and structure of yttria-doped ceria (YDC) have been studied quite extensively.[6−12] Recently, studies using transmission electron microscopy[13,14] and EXAFS[15] have confirmed that the local structure plays an important role in controlling the properties of the materials.

* Corresponding author. Tel: 650-723-4475. Fax: 650-725-2199. E-mail: njkim@stanford.edu.

(1) Inaba, H.; Tagawa, H. *Solid State Ionics* **1996**, *83*, 1.
(2) Kharton, V. K.; Yaremchenko, A. A.; Naumovich, E. N.; Marques, F. M. B. *J. Solid State Electrochem.* **2000**, *4*, 243.
(3) Mogensen, M.; Sames, N. M.; Tompsett, G. A. *Solid State Ionics* **2000**, *129*, 65.
(4) Tuller, H. L.; Nowick, A. S. *J. Electrochem. Soc.* **1975**, *122*, 255.
(5) Mogensen, M.; Lindegaard, T.; Hansen, U. R.; Mogensen, G. *J. Electrochem. Soc.* **1994**, *141*, 2122.
(6) Kudo, T.; Obayashi, H. *J. Electrochem. Soc.* **1975**, *122*, 142.
(7) Dirstine, R. T.; Blumenthal, R. N.; Kuech, T. F. *J. Electrochem. Soc.* **1979**, *126*, 264.
(8) Wang, D. Y.; Park, D. S.; Griffith, J.; Nowick, A. S. *Solid State Ionics* **1981**, *2*, 95.
(9) Fuda, K.; Kishio, K.; Yamauchi, S.; Fueki, K. *J. Phys. Chem. Solids* **1984**, *45*, 1253.
(10) Fuda, K.; Kishio, K.; Yamauchi, S.; Fueki, K. *J. Phys. Chem. Solids* **1985**, *46*, 1141.
(11) Balazs, G. B.; Glass, R. S. *Solid State Ionics* **1995**, *76*, 155.
(12) Tadokoro, S. K.; Porfirio, T. C.; Muccillo, R.; Muccillo, E. N. S. *J. Power Sources* **2004**, *130*, 15−21.
(13) Ou, D. R.; Mori, T.; Ye, F.; Zou, J.; Auchterlonie, G.; Drennan, J. *Electrochem. Solid State Lett.* **2007**, *10*, P1.
(14) Ou, D. R.; Mori, T.; Ye, F.; Takahashi, M.; Zou, J.; Drennan, J. *Acta Mater.* **2006**, *54*, 3737.

10.1021/cm0715388 CCC: $37.00
Published on Web 10/19/2007

Solid-state NMR is becoming increasingly applicable to studies of the local structure and dynamics in oxide ionic conductors. ^{17}O is a spin-5/2 quadrupolar nuclide, and ^{17}O NMR can be particularly useful in some systems, especially when it is combined with NMR of the cation nuclides. YDC was studied by analyzing ^{17}O NMR relaxation times using high-temperature static NMR up to 900 °C,[9,10] and the relaxation times were further analyzed with Monte Carlo simulation.[16] A few static ^{17}O NMR studies of solid oxide conductors to temperatures up to 1000 °C have been reported.[17,18] High-resolution, magic-angle spinning (MAS) studies at intermediate temperatures on bismuth-containing oxide ionic conductors have been described.[19,20] Recently, higher temperature (up to 700 °C) ^{17}O MAS NMR studies were performed on YSZ[21] and several different stabilized zirconias.[22] Although ^{89}Y is a spin-1/2 nuclide, ^{89}Y NMR has not been widely used because of its low gyromagnetic ratio ($\gamma = -1.3155 \times 10^7 \mathrm{radT^{-1}\,s^{-1}}$)[23] and slow spin−lattice (T_1) relaxation.[24] However, occasional ^{89}Y NMR studies have been promising[24−30] and enough information on the relationships between ^{89}Y NMR parameters and structure has appeared to begin to allow the application of this method to investigate the local environments around yttrium. For example, recent studies of ^{89}Y in YSZ[31,32] described details of the Y^{3+} coordination and vacancy distribution over a wide composition range. Here we describe the local structure and dynamics of a series of samples of YDC using ^{89}Y and ^{17}O MAS NMR.

Experimental Section

YDCs with varying yttria contents (5, 10, and 15 mol % Y_2O_3) were prepared by solid-state reactions of pelletized mixtures of Y_2O_3 and CeO_2, heated in air at 1500 °C for 2 to 3 days. Because ^{89}Y NMR is often difficult to carry out due to extremely long spin−lattice relaxation times, another set of YDC samples (5, 10, 15, and 30% Y_2O_3) were synthesized with 0.2 mol % of paramagnetic Gd_2O_3 substituted for ^{89}Y MAS NMR to increase the relaxation rate. For ^{17}O NMR measurements, Gd-free samples were heated in sealed silica glass tubes with 40% ^{17}O-enriched oxygen gas at about 600 °C for 12 h. To confirm that this annealing step did not change the distribution of Y coordinations, fractions of the Gd-doped, 5 and 15% Y_2O_3 samples were also ^{17}O exchanged. The samples were characterized by X-ray diffraction with a Rigaku Geigerflex X-ray diffractometer. Data were compared with the International Centre for Diffraction Data powder diffraction files, which confirmed that all mixtures transformed to the desired cubic phase.

^{89}Y NMR experiments were carried out for the Gd-added YDC with Varian Unity/Inova 600 spectrometer (14.1 T) at a Larmor frequency of 29.39 MHz using a 3.2 mm Varian/Chemagnetics "T3" type MAS probe with a "low gamma box" (external tuning attachment). Spectra were obtained using a single pulse experiment with a typical pulse width of approximately 5 μs, which was the $\pi/2$ radio frequency tip angle, and spinning speeds of 10 kHz. Typically, a 5 s pulse delay was used. T_1 appears to be still several minutes even with Gd doping, although T_1 is significantly reduced compared to estimated T_1 for $Y_2Ti_{0.4}Sn_{1.6}O_7$ (1000−2000 s).[24] Although all the resonances were not fully relaxed with this delay time, no differences in relaxation among different resonances were observed. The chemical shifts were externally referenced to $Y_2Sn_2O_7$ at 150 ppm.[27] The instrumental dead time of about 100 μs was short enough so that spectra were not significantly distorted (line widths of 1 kHz or less); this was confirmed by echo spectra collected on several samples.

^{17}O NMR data were collected with Varian Infinity Plus 400 (9.4 T) and Unity/Inova 600 and 800 (14.1, 18.8 T) spectrometers at Larmor frequencies of 54.19, 81.31, and 108.38 MHz, respectively. Single pulse spectra were acquired using 3.2 mm Varian/Chemagnetics "T3" type MAS probes with spinning speeds of about 20 kHz. A small pulse width was used to ensure that the intensities are quantitative for ^{17}O, a quadrupolar nuclide. A typical pulse width was 0.3 μs, equivalent to a $\pi/18$ rf tip angle for the liquid standard. The chemical shifts were externally referenced to ^{17}O-enriched water at 0 ppm at ambient temperature.

Data up to 150 °C were collected with a 4 mm Varian/Chemagnetics "T3" type MAS probe with a spinning speed of about 15 kHz at 9.4 T. The pulse width was 0.4 μs ($\pi/18$ rf tip angle). Experiments to 500 °C were carried out at 9.4 T with a high-temperature MAS probe with 7 mm Si_3N_4 rotors (Doty Scientific, Inc.) at a spinning speed of 5 kHz. A typical pulse width was 0.3 μs ($\pi/36$ rf tip angle). The temperatures were checked using $Pb(NO_3)_2$ between the room temperatures and 400 °C for both probes. The estimated accuracies of temperature are about 10 °C for the 7 mm probe and about 5 °C for 4 mm probe. The number of acquisitions was typically 1500 to 3000 for the 7 mm probe and 5000 for the 4 mm probe with a pulse delay of 1 s. The probe dead time was typically less than 20 μs.

Results and Discussion

X-ray Diffraction. The X-ray diffraction patterns showed that the doped cerias had the cubic fluorite structure throughout the range from 5 to 30% Y_2O_3. Unit cell parameters of the YDCs (Gd-added and Gd-free) are shown in Figure 1. The unit cell lengths of both sets of samples increased as yttrium contents decreased, indicating that yttrium does enter into the cubic fluorite structure of the ceria. The volume of the unit cell decreases due to the vacancies generated by yttrium doping, although the size of the yttrium ion is larger than that of the cerium ion.[33,34]

(15) Wang, Y. R.; Kageyama, H.; Mori, T.; Yoshikawa, H.; Drennan, J. *Solid State Ionics* **2006**, *177*, 1681.
(16) Adler, S. B.; Smith, J. W.; Reimer, J. A. *J. Chem. Phys.* **1993**, *98*, 7613.
(17) Adler, S. B.; Reimer, J. A.; Baltisberger, J.; Werner, U. *J. Am. Chem. Soc.* **1994**, *116*, 675.
(18) Adler, S. B.; Reimer, J. A. *Solid State Ionics* **1996**, *91*, 175.
(19) Kim, N.; Grey, C. P. *Science* **2002**, *297*, 1317.
(20) Kim, N.; Vannier, R. N.; Grey, C. P. *Chem. Mater.* **2005**, *17*, 1952.
(21) Viefhaus, T.; Bolse, T.; Muller, K. *Solid State Ionics* **2006**, *117*, 3063.
(22) Kim, N.; Hsieh, C.-H.; Huang, H.; Prinz, F. B.; Stebbins, J. F. *Solid State Ionics*, in press.
(23) Harris, R. K. *Nuclear Magnetic Resonance Spectroscopy*; Pitman: London, 1983.
(24) Ashbrook, S. E.; Whittle, K. R.; Lumpkin, G. R.; Farnan, I. *J. Phys. Chem. B* **2006**, *110*, 10358.
(25) Thompson, A. R.; Oldfield, E. *J. Chem. Soc., Chem. Commun.* **1987**, 27.
(26) Battle, P. D.; Montez, B.; Oldfield, E. *J. Chem. Soc., Chem. Commun.* **1988**, 584.
(27) Grey, C. P.; Smith, M. E.; Cheetham, A. K.; Dobson, C. M.; Dupree, R. *J. Am. Chem. Soc.* **1990**, *112*, 4670.
(28) Gautier, N.; Gervais, M.; Landron, C.; Massiot, D.; Coutures, J.-P. *Phys. Status Solidi A* **1998**, *165*, 329.
(29) Florian, P.; Gervais, M.; Douy, A.; Massiot, D.; Coutures, J.-P. *J. Phys. Chem. B* **2001**, *105*, 379.
(30) Kim, N.; Grey, C. P. *Dalton Trans.* **2004**, 3048.
(31) Kawata, K.; Maekawa, H.; Nemoto, T.; Yamamura, T. *Solid State Ionics* **2006**, *177*, 1687.
(32) Henson, L. J.; Darby, R. J.; Kumar, R. V.; Farnan, I. *Abstracts, 2006 MRS Fall Meeting, Boston, MA, Nov. 27-Dec. 1*, **2006**.

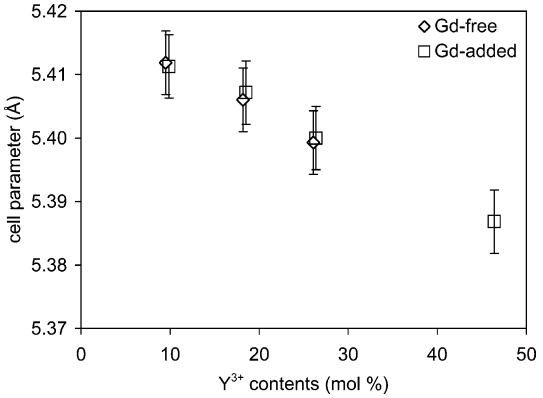

Figure 1. Unit cell parameters for Y_2O_3-doped CeO_2, comparing samples with and without 0.2% Gd_2O_3. Note that Y^{3+} concentrations are used instead of those of Y_2O_3 because the cell parameters are expected to be dependent on the dopant cation concentration.

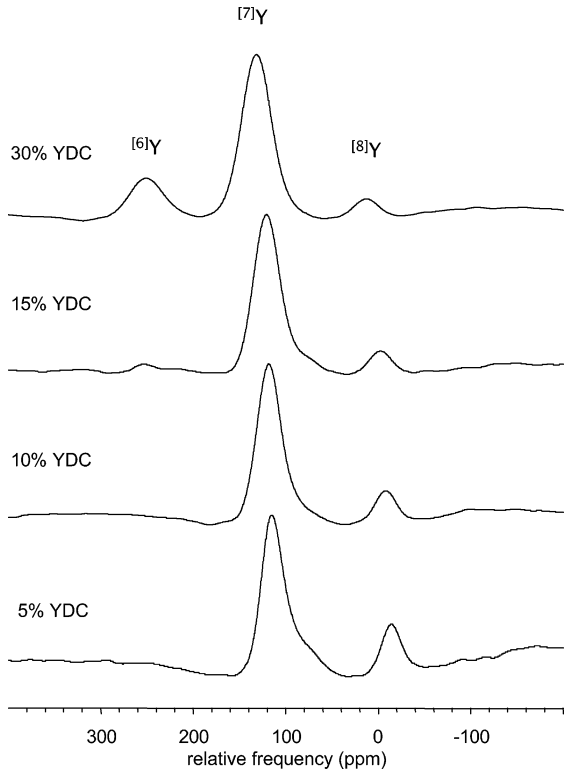

Figure 2. ^{89}Y MAS NMR spectra (14.1 T) of Gd-added Y_2O_3-doped CeO_2. Y coordinations are marked. The spinning speed of 10 kHz is sufficient to place all spinning sidebands outside of the region shown.

^{89}Y MAS NMR. The ^{89}Y MAS NMR spectra of the Gd-added YDC samples (Figure 2) show two or three resonances centered at about 0, 120, and 250 ppm, depending on the Y_2O_3 content. Spectra for two samples annealed at 600 °C for ^{17}O exchange were essentially identical to unannealed samples of the same compositions. The predominant effect on the ^{89}Y chemical shift (the same as the peak position for this spin-1/2 nuclide) is the first shell coordination number, which ranges from six to eight for yttrium in most crystalline oxides. The chemical shift increases as the coordination number decreases, according to previous ^{89}Y NMR studies, for example 270 and 315 ppm for the two six-coordinated yttrium sites in Y_2O_3[25] and 150 and 65 ppm for eight-coordinated yttrium sites in pyrochlores, $Y_2Sn_2O_7$ and $Y_2Ti_2O_7$.[27] This trend is similar to those found for many other NMR nuclei such as ^{11}B, ^{23}Na, ^{25}Mg, ^{27}Al, ^{29}Si, and ^{45}Sc.[35,36] Therefore, the three resonances can be assigned to six-, seven-, and eight-coordinated yttrium sites from high to low frequency. A similar assignment pattern was made for three peaks in ^{89}Y spectra of a range of compositions of YSZ, i.e., 85−90, 190−195, and 300−305 ppm were assigned to six-, seven-, and eight-coordinated sites, respectively.[31]

As the Y_2O_3 content is increased, there are systematic changes in the spectra. For example, the positions of all three resonances are shifted to higher frequency. The chemical shift of ^{89}Y is known to be sensitive not only to oxygens in the first coordination shell but also to cations in the second shell.[27] Therefore, as yttrium content increases, the number of yttriums in the second shell increases, probably causing the observed changes in peak position. Eventually, if there are even more yttrium cations in the second shell, the structure will become similar to that of C-type Y_2O_3, which has two yttrium sites whose chemical shift values are 315 and 270 ppm,[25] higher than the value of 255 ppm observed for six-coordinated yttrium in the 30% YDC. It is also possible that the overall change in unit cell size contributes to the observed changes in ^{89}Y chemical shifts. Similar to the effect of coordination number, a bond distance decrease could shift the peak position to a higher frequency as the Y^{3+} content is increased. However, the effect of bond distance on the chemical shift is not fully understood; moreover, chemical shifts of each coordination environment do not change much with unit cell size in YSZ.[31]

The line width also increases with the Y_2O_3 content: about 600 Hz (20 ppm) at the 5% dopant level to 1 kHz (34 ppm) at the 30% dopant level. Since doping of Y^{3+} generates vacancies, one can expect the structure to become more disordered due to distributions in bond distances and angles. At the lower dopant levels, a low frequency shoulder is clearly seen on the largest peak (seven-coordinated Y). The shoulder appears to be present for the composition from 5 to 15% with decreasing intensity, although it is difficult to quantify due to the change in the line width of the main peak. The shoulder can probably be attributed to a difference in the cations in the second coordination sphere. Given that each cation has twelve cation neighbors, this feature could be due to Y with no Y neighbors instead of one (or more) Y neighbors, as represented by the main peak. On the other hand, a Gd neighbor cation(s) could also cause a change in peak position and thus the shoulder. Although the overall doping level of Gd_2O_3 is only 0.2 mol %, the Gd/Y ratio for 5% YDC is 0.04, leading to a possibly detectable level of perturbations from one or more Gd cation neighbors.

The most structurally revealing changes with composition in the ^{89}Y spectra involve the relative peak intensities: the higher frequency peaks grow and the lower frequency peaks decrease as Y_2O_3 content increases. The relative proportions of the eight-, seven-, and six-coordinated sites, determined

(33) Glushkova, V. B.; Hanic, F.; Sazonova, L. V. *Ceramurgia Int.* **1978**, *4*, 176.
(34) Kim, D.-J. *J. Am. Ceram. Soc.* **1989**, *72*, 1415.
(35) MacKenzie, K. J. D.; Smith, M. E. *Multinuclear Solid-State NMR of Inorganic Materials*; Pergamon: New York, 2002.
(36) Kim, N.; Hsieh, C.-H.; Stebbins, J. F. *Chem. Mater.* **2006**, *18*, 3855.

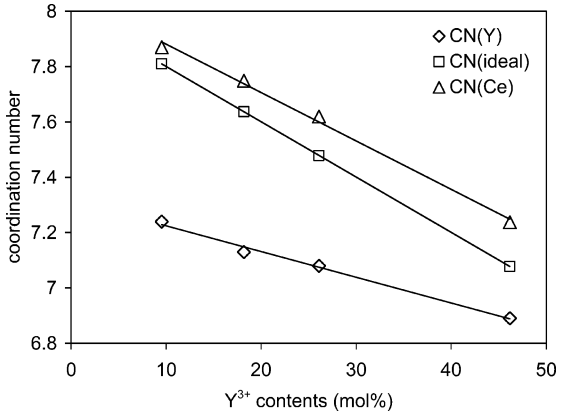

Figure 3. Effects of dopant content on the average coordination number of Y^{3+} cations, as measured by ^{89}Y NMR, CN(Y); comparison with the ideal, mean overall cation coordination number derived from the composition and total vacancy content, CN(ideal); and derived mean coordination number of Ce^{4+}, CN(Ce). Note that Y^{3+} concentrations are used instead of those of Y_2O_3 for consistency with Figure 1.

Table 1. Peak Positions and Relative Areas of Peaks in ^{89}Y MAS NMR Spectra of Gd-Added YDC, Which Represent Cations with the Coordinations Shown

			$^{[6]}Y$		$^{[7]}Y$		$^{[8]}Y$	
Y_2O_3, mol %	Y^{3+}, mol %	vacancies, mol %	peak, ppm	area, %	peak, ppm	area, %	peak, ppm	area, %
5	9.5	2.4			117	76	−14	24
10	18.2	4.5			119	87	−10	13
15	26.1	6.5	255	2	120	88	−6	10
30	46.2	11.5	255	17	130	77	10	6

by integration, are given in Table 1. The average coordination number of Y^{3+}, CN(Y), was calculated for each composition using the formula

$$\mathrm{CN(Y)} = \sum^{n}(I_n n) \tag{1}$$

where I_n is relative area of the ^{89}Y MAS NMR peak for the n-coordinated site. The observed average yttrium coordination numbers were then compared with the ideal coordination numbers, CN(ideal), which were calculated for a random distribution using the equation

$$\mathrm{CN(ideal)} = 8(1 - R) \tag{2}$$

where R is the oxygen vacancy concentration. The average coordination number of Ce, CN(Ce), can then be calculated from CN(Y) and CN(ideal), as the latter must be equal to the average for all cations:

$$\mathrm{CN(ideal)} = (1 - x)\,\mathrm{CN(Ce)} + x\mathrm{CN(Y)} \tag{3}$$

$$\mathrm{CN(Ce)} = \frac{\mathrm{CN(ideal)} - x\mathrm{CN(Y)}}{1 - x} \tag{4}$$

where x is molar ratio of Y^{3+} to total cations.

The estimated coordination numbers are plotted versus composition in Figure 3. The observed average coordination numbers of Y^{3+} are considerably lower than the ideal values for the entire composition range investigated, which indicates that vacancies have a higher probability of being located adjacent to yttrium cations than to cerium cations. When the dopant content is low this difference is more pronounced. Although it is difficult to completely rule out the possibility

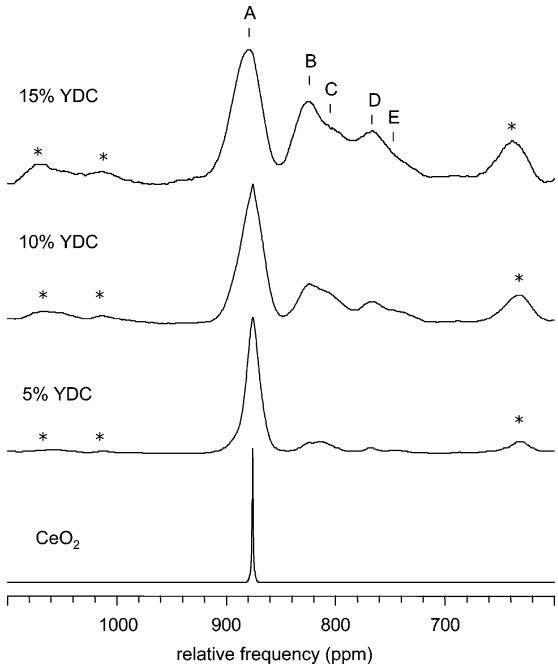

Figure 4. ^{17}O MAS NMR of Y_2O_3-doped CeO_2 at 14.1 T with a spinning speed of 20 kHz. Spinning sidebands are marked by asterisks. As discussed in the text, peak A is assigned to oxygen with 4 Ce neighbors, peaks B and C to oxygen with 3 Ce and 1 Y neighbor, and peaks D and E to oxygen with 2 Ce and 2 Y neighbors.

of the formation of clusters resembling ordered C-type Y_2O_3, the ^{89}Y chemical shift of the six-coordinated site in YDC (about 250 ppm) is still quite different from those of Y_2O_3 (270 and 315 ppm) and thus any contribution of Y_2O_3 to the total intensity must be below detection limits of about 2%.

^{17}O MAS NMR. The ^{17}O MAS NMR spectrum of pure ceria (Figure 4) shows one resonance at 877 ppm, consistent with previous results.[37] This peak is exceptionally narrow (<1 ppm) and has very small spinning sidebands, as expected from its ordered cubic structure, in which each oxygen anion has true cubic local symmetry and therefore a quadrupolar coupling constant of zero. The ^{17}O MAS NMR spectra of all of the YDC samples show at least five resonances with much broader line widths. Spectra from two different fields (14.1 and 18.8 T) do not show any significant differences in line width, indicating that widths are dominated by chemical shift distributions with only a small quadrupolar interaction. This is expected from the mainly ionic nature of the bonds, even when the local structure is asymmetric due to varying cation neighbors. The five partially resolved resonances, labeled A through E, are centered at about 877, 826, 812, 768, and 743 ppm respectively. These can be divided into three groups (A, B + C, D + E). Because of severe overlap of the components of the latter two pairs, we report the relative areas of only the three groups in Table 2.

The largest contribution to the ^{17}O chemical shift is again expected to be the first shell coordination environment, i.e., oxygen with 4 Ce neighbors, 3 Ce + 1 Y neighbor, etc. Effects from various cations on ^{17}O chemical shifts are often approximately additive.[38] Because the shift for four-

(37) Bastow, T. J.; Stuart, S. N. *Chem. Phys.* **1990**, *143*, 459.
(38) Kim, N.; Grey, C. P. *J. Solid State Chem.* **2003**, *175*, 110.

Table 2. Relative Areas of Peaks in ^{17}O MAS NMR Spectra of YDC, Compared with the Populations of Oxygen Coordination Environments Based on a Random Distribution of Cations[a]

	measured areas, %			calculated populations, %				
Y_2O_3, mol %	A	B + C	D + E	Ce4	Ce3Y1	Ce2Y2	Ce1Y3	Y4
5.0	81	14	5	81.45	17.15	1.35	0.05	0.00
10.0	64	26	10	65.61	29.16	4.86	0.36	0.01
15.0	50	35	15	52.20	36.85	9.75	1.15	0.05

[a] Peak A is assigned to Ce4, B + C to Ce3Y1, and D + E to Ce2Y2.

coordinated oxygen sites in CeO_2 is 877 ppm and those of four-coordinated oxygen sites in Y_2O_3 are 346−383 ppm,[39] the three groups of resonances, A, B + C and D + E, can thus be assigned to oxygens with 4 Ce, 3 Ce + 1 Y, and 2 Ce + 2 Y, respectively, and are denoted as Ce4, Ce3Y1, and Ce2Y2 below. The populations of oxygen sites with 1 Ce or no Ce appear to be negligible, as no other peaks were detected. The relative populations of these different oxygen coordination environments are shown in Table 2.

The two overlapped components of the B/C and D/E pairs are probably related to discrete differences in the second shell, most likely the presence or absence of an oxygen vacancy adjacent to one of the coordinating Y^{3+} cations. Because the ^{89}Y data indicate that vacancies are less common adjacent to Ce^{4+}, this peak splitting is much less prominent for the A peak, which has all Ce neighbors and thus a lower probability of a vacancy in the second shell. Nonetheless, the marked broadening of the A peak with increasing Y_2O_3 content could be related to the higher vacancy content, as cerium-vacancy pairs certainly are present (the mean coordination number of Ce is <8 for all YDCs, Figure 3) and thus contribute to the disorder in all local oxygen environments. A second-shell vacancy, which reduces the coordination number of a first-shell cation, might be expected to result in a slightly shorter bond to that cation. In simple cases such as alkaline earth oxides,[40] such a change would be expected to lead to a lower chemical shift. However, the A peak shifts to a slightly higher frequency with increasing Y_2O_3, suggesting that details of ^{17}O chemical shift systematics in YDC may be more complex.

Although the distribution of vacancies may not be easy to quantify in detail, the cation distribution can be investigated by comparing the relative intensities of A, B + C, and D + E with the populations of Ce4, Ce3Y1, and Ce2Y2 calculated for a random distribution of cations. The relative intensity of A is similar to the population of Ce4, and accordingly the sum of B + C + D + E is similar to the sum of Ce3Y1 and Ce2Y2, suggesting that yttrium is not segregated in the structure. However, the relative proportion of Ce2Y2 sites (D + E) is significantly higher than that calculated for the random model, indicating that the probability of pairs of Y^{3+} is higher than in the random distribution. This finding is consistent with the ^{89}Y MAS NMR results, where the average coordination number of Y is lower than that in a random distribution, which also suggested the possibility of two yttriums pairing with one vacancy. The ratio between measured intensities of B + C and D + E decreases with Y content less rapidly than in the random model, but the calculated population of Ce2Y2 increases considerably as Y content is increased.

This observation is similar to a conclusion reached in a recent ^{45}Sc MAS NMR study of Sc^{3+} coordination in scandia-stabilized zirconia (SSZ), which suggested that two scandiums pair with one oxygen vacancy.[36] On the other hand, it is quite different from recent ^{89}Y MAS NMR studies of YSZ,[31,32] where the average coordination number of Y^{3+} appeared to be higher than that of Zr^{4+}, suggesting that vacancies are found more frequently next to zirconium than to yttrium.

This contrast in ordering effects probably arises from the differences in size between the host and the dopant cations. In general, larger cations tend to favor longer bonds to oxygen anions and thus higher coordination numbers. However, the behavior of aliovalent dopant cations may be less straightforward due to the charge difference and oxygen vacancies. Although the dopant cations, Sc^{3+} and Y^{3+} (r = 0.87, 1.019 Å[41]), are slightly larger than the host cations, Zr^{4+} and Ce^{4+} (r = 0.84, 0.97 Å), in SSZ and YDC, respectively, dopants and vacancies still have a strong tendency to associate, reducing the coordination number of the dopant. Therefore, for a dopant to have the higher coordination number, its size apparently needs to be much larger than that of the host cation.

Similar observations are found in the relation between the size of the unit cell and the size of the dopants. It has also been suggested that ionic conductivity should be high when the radius of the dopant matches the critical radius (r_c), a radius for a dopant with a given charge for which doping does not change the unit cell size.[34] In the case of SSZ and YDC, although Sc^{3+} and Y^{3+} are larger than the host cations, Zr^{4+} and Ce^{4+}, they are still smaller than the r_c's, which for trivalent dopants are 0.948 for Zr^{4+} and 1.038 Å for Ce^{4+}.[34] For YSZ, on the other hand, Y^{3+} is larger than r_c and thus a mean coordination number for Zr^{4+} that is higher than that of Y^{3+} appears to be favored. The association between dopant and vacancies thus seems to still be significant when the dopant size is smaller than the critical radius.

High-Temperature ^{17}O MAS NMR. For 5% YDC, ^{17}O MAS NMR spectra were collected up to 500 °C at a spinning speed of 5 kHz with a special high-temperature probe (Doty Scientific, Inc.) and up to 150 °C at a 20 kHz spinning speed with a Varian/Chemagnetics 3.2 mm T3 probe (Figure 5). In the slower spinning speed spectra, although not all the resonances are as clearly resolved as in the spectra with faster spinning, the beginning of coalescence among the peaks is clearly observed at about 200 °C, with complete motional averaging and peak narrowing above 400 °C. The chemical shift at temperatures above the coalescence point, which represents the weighted average of the resonances of all exchanging oxygens, is 854 ppm, close to the center of gravity of all the resonances at room temperature of about 860 ppm. Except for a small amount of a pure CeO_2 impurity

(39) Florian, P.; Massiot, D.; Humbert, G.; Coutures, J.-P. *C. R. Acad. Sci. Paris, Ser. IIb* **1995**, *320*, 99.
(40) Turner, G. L.; Chung, S. E.; Oldfield, E. *J. Magn. Reson.* **1985**, *64*, 316.
(41) Shannon, R. D. *Acta. Crystallogr.* **1976**, *A32*, 751.

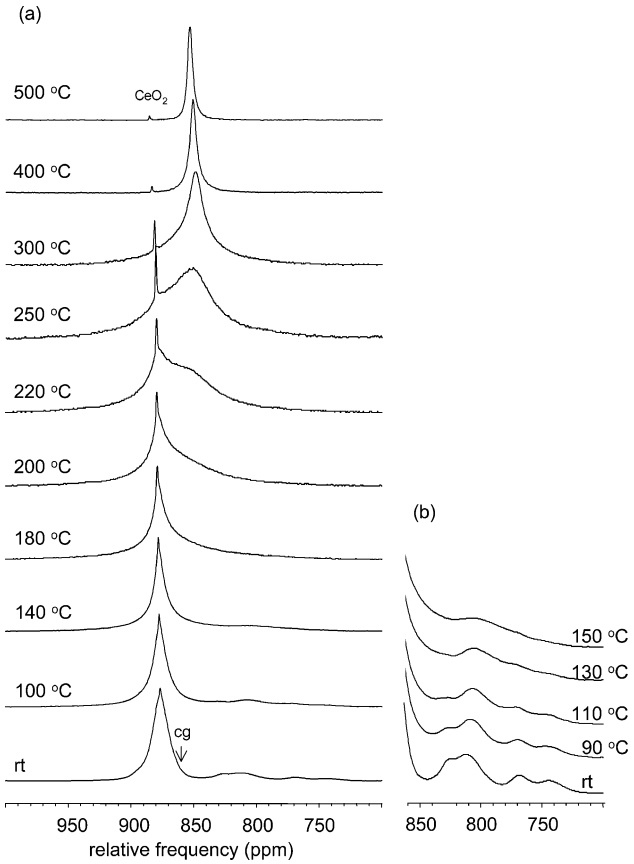

Figure 5. High-temperature ^{17}O MAS NMR spectra of 5% Y_2O_3-doped CeO_2 at 9.4 T with a spinning speed of (a) 5 kHz and (b) 20 kHz. The center of gravity of all the resonances at room temperature (about 860 ppm) is labeled as cg. In (a), a small, very narrow peak for a pure CeO_2 impurity appears to grow in intensity in the mid-temperature range only because the width of the main peak is at its maximum in this region, and spectra are normalized to the maximum peak height.

(which is prominent because of its extremely narrow peak), all resonances coalesce to one peak at high temperature. This indicates that all the oxygens in the structure are exchanging and there are no clusters with locally different structure that are abundant enough to be detectable by NMR. The spectral separation of the resonances is about 7 kHz, indicating that the mean exchange frequency of oxygens among sites with varying numbers of Ce and Y neighbors reaches 44 kHz ($\sim 2\pi\Delta\nu$; $\Delta\nu$ is spectral separation) when coalescence becomes marked.

The spectra with faster spinning speeds, and thus higher resolution (Figure 5b), show that coalescence begins at lower temperatures for the lower frequency peaks, becoming quite noticeable at 110 °C. These peaks were assigned to the oxygens that have one or two yttriums in the first coordination sphere. The chemical shift of the averaged peak at 150 °C is about 805 ppm, which is consistent with the center of the gravity of peaks B through E. The spectral separation between B and E is about 4.5 kHz, and thus the estimated mean exchange rate is approximately 28 kHz. It thus appears that exchange of oxygens among sites with one or two Y neighbors becomes significant at a lower temperature than exchange among all sites, including those with no Y neighbors. This may be expected from our finding that vacancies have some preference to be located next to Y cations. However, because of this association between dopant cations and vacancies, these more rapid jumps may be restricted to a short range around dopant cations and may thus contribute less to the long-range oxygen migration.

Conclusions

Local structure and oxygen dynamics in YDC were studied using ^{89}Y and ^{17}O MAS NMR at ambient and high temperatures. Data for both nuclides suggest that the cation and vacancy distributions are not random. In the ^{89}Y spectra, yttrium cations with different coordination numbers were clearly identified, and their relative proportions quantified. These results show that the average coordination number of yttrium is smaller, and that of cerium is larger, than the average coordination number that is dictated by the composition and total vacancy content. This indicates that the oxygen vacancies and the dopant cations are associated more than predicted from a random distribution. The relative abundances of oxygen sites with zero, one, and two Y neighbors, as determined from ^{17}O NMR, suggests also the possibility of two yttriums pairing with one vacancy. This behavior is similar to that of scandium cations in scandium stabilized zirconia,[36] but is opposite to that of yttrium cations in yttrium stabilized zirconia.[31] High-temperature ^{17}O MAS NMR shows that oxide anion jumps between sites with yttrium neighbors become prominent at somewhat lower temperatures than those at which oxygen exchange throughout the structure develops.

Acknowledgment. We thank the Stanford Global Climate and Energy Project (GCEP) for financial support and Stanford Magnetic Resonance Laboratory for access to the 18.8 T NMR spectrometer.

CM0715388